Proc. of SPIE Vol. 1533, Optomechanics and Dimensional Stability, ed. R A Paquin, D Vukobratovich (Dec 1991) Copyright SPIE

Interference Fit Equations for Lens Cell Design

Ralph M. Richard and Tina M. Valente
Optical Sciences Center
University of Arizona
Tucson, Arizona 85721

ABSTRACT

Optical designs often consist of lenses which are mounted in a common lens barrel. One method for mounting these lenses is to mount each individual lens in its own subcell using an adhesive and then use an interference or press fit to mount these subcells in the lens barrel. When mounting lenses in this manner, it is necessary to evaluate the stress induced in the glass and the residual difference in the optical path. A closed form analytical derivation was made for a simple lens mount which relates the allowable magnitude of the interference fit to the stress in the glass. This theoretical expression was modified using finite element models in order that it may be used for complex lens designs. Proper modeling such as element material properties are addressed as well as applications for various mounting conditions.

1. INTERFERENCE FIT EQUATIONS

The equations which give the displacements and stresses between and interior to cylinders which are force fitted are derived from compatibility and equilibrium considerations used in the theory of elasticity. Shown in Figure 1 is a cross section of a short cylinder of length l_i that is force fitted into a longer cylinder of length l_o. For the case where l_o is equal to l_i and the cylinders are of the same material, the following equation gives the relation between the interference and the interface pressure (1).

$$\delta = \frac{4\,b^3\,(c^2 - a^2)}{(b^2 - a^2)(c^2 - b^2)}\,\frac{p}{E} \tag{1}$$

where:

δ = interference fit between the two cylinders
p = pressure between the two cylinders
E = Young's modulus of the material
a,b,c = cylinder radii shown in Figure 1.

For the usual geometries of subcells (inner cylinder) which are mounted in a common lens barrel (the outer cylinder), the radii a, b, and c are approximately equal since the subcell and lens barrel are thin. Using the approximation $a \simeq b \simeq c$ in Equation 1 gives:

$$\delta = \frac{2\,p\,b^2}{E}\left[\frac{1}{t_o} + \frac{1}{t_i}\right] \tag{2}$$

where t_o and t_i are the thicknesses of the outer and inner cylinders, respectively. The radial displacement inward of the inner cylinder as shown in Figure 1 is (1)

$$u_1 = \frac{p\,b^2}{E\,t_i} \tag{3}$$

Using Equation 1, this radial displacement may be determined as a function of the interference fit, i.e.,

$$u_1 = \left[\frac{\delta}{2}\right] \frac{t_o}{t_o + t_i} \tag{4}$$

Equations 1 through 4 apply only when the inner cylinder is the same length as the outer cylinder. However, in barrel mounted lenses the inner cylinder which represents the subcell is shorter than the barrel as shown in Figure 1. To model this latter case, Equation 4 is modified by introducing an *effective thickness* of the inner cylinder,

$$t_i^* = \beta\, t_i \tag{5}$$

where β is a function of l_o and l_i which are the lengths of the outer and inner cylinders, respectively. Using finite element models of the two cylinder system of Figure 1, the β function of Equation 5 was found empirically to solve this axisymmetric elasticity problem.

$$\beta = 0.44 \left\{ 1 - \frac{1}{2}\left[\frac{l_i}{l_o}\right] + \frac{7}{4}\left[\frac{l_i}{l_o}\right]^2 \right\} \tag{6}$$

2. SUBCELL STRAINS, STRESSES, AND DISPLACEMENTS

Shown in Figure 2 is a typical barrel lens mount. It comprises a lens mounted in a metal ring using an elastomer annulus. This assembly is then force fitted into the barrel tube.

If Young's modulus of the elastomer is much less than that of the glass lens and the metal ring, the radial displacement at the outer boundary of the elastomer is given by Equation 4 modified by Equations 5 and 6.

$$u_r = \left[\frac{\delta}{2}\right] \frac{t_o}{t_o + t_i^*} \tag{7}$$

The radial strain in the elastomer is

$$\epsilon_r = \frac{u_r}{t_e} \tag{8}$$

where t_e is the radial thickness of the elastomer.

If the elastomer is thin relative to the lens thickness, the radial stress in the elastomer is (2),

$$\sigma_r = \frac{E_e\, \epsilon_r}{1 + \nu_e}\left[1 + \frac{\nu_e}{1 - 2\,\nu_e}\right] \tag{9}$$

where:

E_e = Young's modulus of the elastomer
ν_e = Poisson's ratio of the elastomer

However, if the elastomer is not thin relative to the lens thickness, the radial stress in the elastomer is (2),

$$\sigma_r = \frac{E_e \epsilon_r}{(1 - \nu_e^2)} \tag{10}$$

Finite element analyses indicated Equations 7 through 9 are accurate to within 8 percent for a glass lens mounted in metal rings with elastomers having a Young's modulus less than 50,000 psi. If Young's modulus of the elastomer is not much less than the glass lens and metal ring, finite element analyses indicate that the β function of Equation 5 should be further modified as follows:

$$\beta^* = \beta (1 + 5.4 \times 10^{-5} E_e) \tag{11}$$

The radial stress on the boundary of the lens is approximately equal to elastomer radial stress. It is this lens stress which may be used to compute the optical path difference due to the glass stress.

3. VERIFICATION USING FINITE ELEMENT MODELING

In order to verify the semi-emperical formulation, finite element interference fit models were constructed using the GIFTS program. Shown in Figure 3 is one of the many axisymmetric finite element models used. A lens is held in a ring mounting with epoxy which is then pressed into an outer ring. For this model the lens has a radius of 5 inches, a thickness of 1 inch, and the following material properties: $E = 10 \times 10^6$ psi, $\nu = .17$. Both the inner and outer rings have the properties of steel ($E = 30 \times 10^6$ psi, $\nu = .30$) and a thickness of .15 inches. The layer of epoxy has a thickness of .20 inches. This is a representative thickness recommended for many epoxies when mounting optics of this size.

The factors that have the greatest influence on the stress induced by one of these mounting schemes are the epoxy properties and the li/lo ratios. To investigate the effects of the epoxy properties, a study was conducted where the diametrical interference and the li/lo ratio were held constant. Young's modulus of the epoxy was varied from 500 psi to 50,000 psi with a Poisson's ratio of 0.41. The results of this study are shown in Figure 4. There is good agreement between the finite element results and the analytical solution when the Young's modulus of the epoxy is less than 10 percent that of the mounting rings. It is also noted that the calculated stress does not vary linearly with the Young's modulus of the epoxy.

The effects of varying the length of the mounting tubes (li/lo) were also studied. As in the previous study, the diametrical interference was held constant as was the properties of the epoxy ($E = 500$psi, $\nu = 0.41$). The values for li/lo were varied from 1 to 8 to obtain the results tabulated in Figure 5. For all cases, there was good agreement between finite elements and semi-empirical solutions (less than 8 percent error). This study showed that changing the ratio of li/lo had a lesser effect on the stresses compared to the impact of epoxy properties. Manufacturers and suppliers of elastomers are often unable or reluctant to specify the precise mechanical properties (E, ν, and G) of the elastomer due to the variabilities which result from temperature, humidity, curing environment, etc. For this reason it is often advisable to perform parametric studies to assess the effects of these variables.

4. OPTICAL PATH DIFFERENCE

The stress induced in the glass when the lenses are mounted with an interference fit influences the refraction index of the element. The following relationship can be used to relate the optical path difference due to the glass stress:

$$\Delta = K \times a \times \sigma \tag{12}$$

where:

K = Stress optical coefficient
a = Lens thickness (light path in medium)
σ = Tensile or compressive stress

This coefficient K, which is derived from the relationship between effective stress and optical path difference that results from stress-induced birefringence, is a material constant. This stress optical coefficient of glass is typically determined from a uniaxial stress test. Equation 12 is a simplified approximation for this case; the stress optical coefficient for various glasses as well as a more detailed description of this formula, can be found, for example, in the Schott-Glass catalog (3).

5. ACKNOWLEDGEMENTS

This study was partially funded by a contract with the U. S. Naval Observatory. The authors would also like to thank Daniel Vukobratovich for his helpful suggestions for this paper.

6. REFERENCES

1. Wang, C. T., *Applied Elasticity*, McGraw Hill Book Company, 1953.

2. Volterra, E. and Gaines, J.H., *Advanced Strength of Materials*, Prentice-Hall, Inc., 1971.

3. Schott-Glass Catalog, Schott-Glass Technologies, Inc., 400 York Ave., Duryea, Penn., 1989.

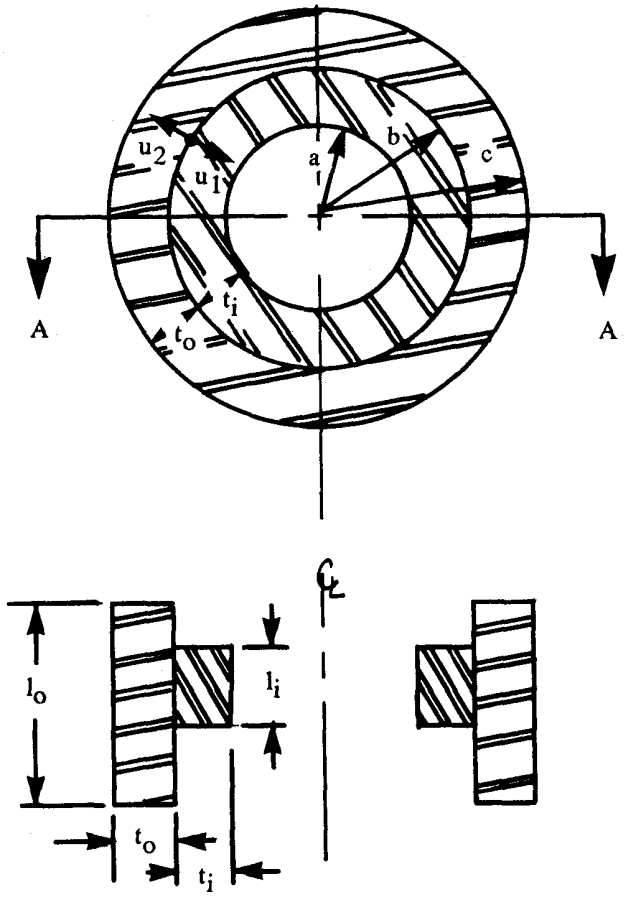

Section A - A

Figure 1. Force fitted cylinders to model a barrel lens mount

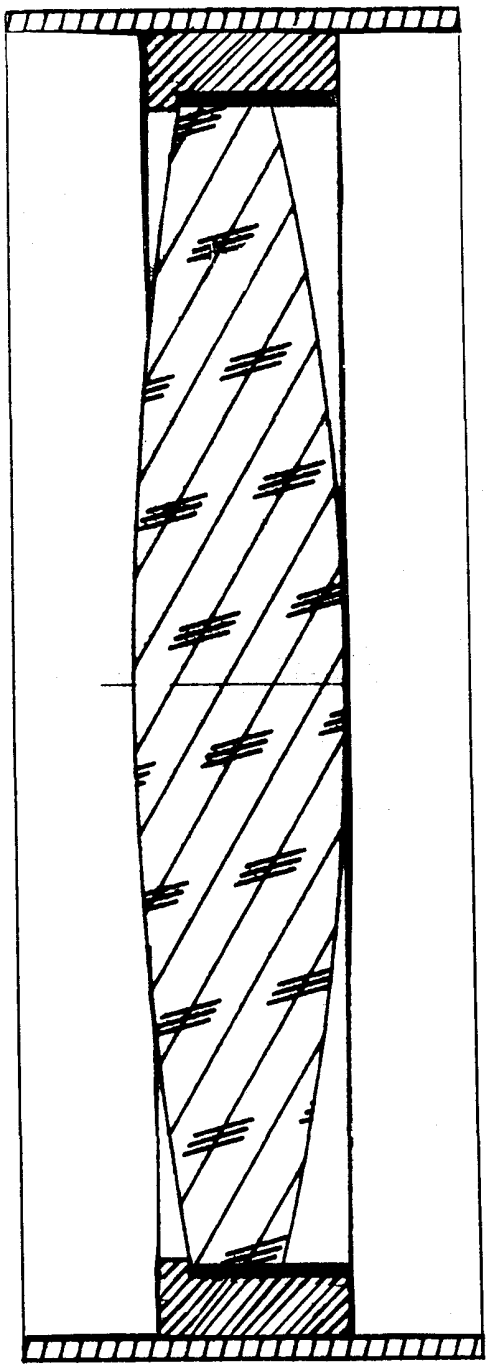

Figure 2. A typical barrel lens mount

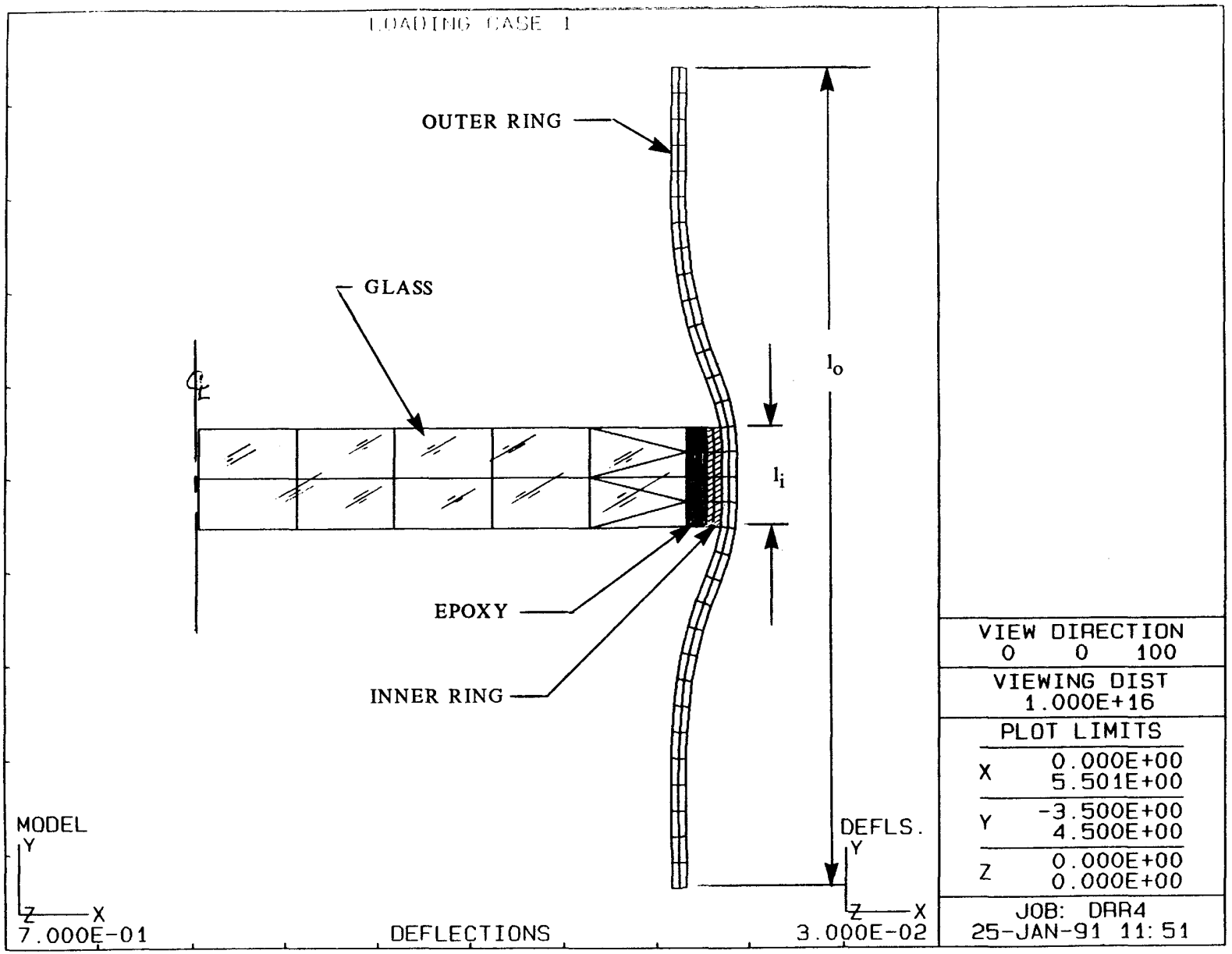

Figure 3. Axisymmetric finite element interference fit model

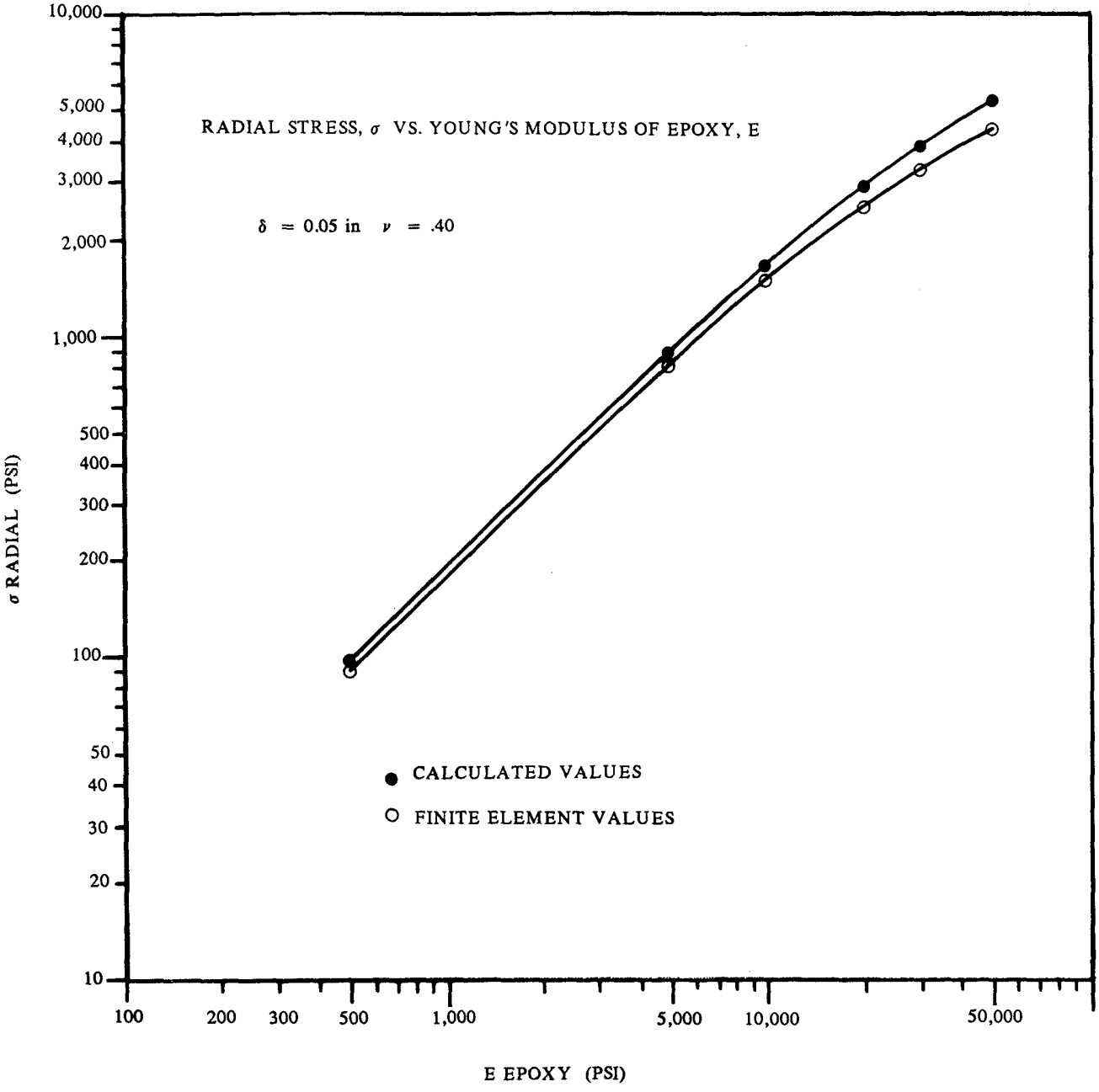

Figure 4. Radial stresses for varying values of Young's modulus of the epoxy

δ = 0.05 in. E Epoxy = 500 psi ν = .40

$\frac{li}{lo}$	u radial (in)	t_i^* (eff)	σ radial (eq. 9) (psi)	σ radial (F.E.) (psi)	Error between methods
.125	.0174	.064	93.27	88.80	5 percent
.167	.0174	.064	93.27	88.70	5 percent
.250	.0173	.065	92.73	87.30	6 percent
.500	.0163	.078	87.16	82.90	5 percent
1.00	.0124	.150	66.43	62.50	6 percent

Figure 5. Radial stress for varying tube length ratio $\left[\frac{lo}{li}\right]$